J Membrane Biol (2010) 237:41–49
DOI 10.1007/s00232-010-9301-2

Effect of Membrane Structure on the Action of Polyenes II: Nystatin Activity along the Phase Diagram of Ergosterol- and Cholesterol-Containing POPC Membranes

J. González-Damián · I. Ortega-Blake

Received: 16 November 2009 / Accepted: 27 August 2010 / Published online: 25 September 2010

Abstract Pores formed by the polyene antibiotic nystatin were studied in solvent-free lipid membranes. The membranes were formed by the tip-dip technique using 1-palmitoyl-2-oleoyl-*sn*-glycero-3-phosphocholine (POPC) with different mol fractions (0–50%) of cholesterol or ergosterol. The effects of the mol fraction of sterol and of temperature variation (15–35°C) on the activity of the pores, their unitary conductances, lifetimes and time average conductances were studied. The results were used to analyze the behavior of nystatin channels along the phase diagrams previously reported for these lipid mixtures and to propose that membrane structure is the determinant factor for the known ergosterol/cholesterol selectivity.

Keywords Nystatin · Permeability model · Membrane structure · Cholesterol · Ergosterol

Introduction

In recent years there has been growing interest in understanding the role that lipid bilayer structure has on the action of transmembrane biomolecules (Phillips et al. 2009; Schmidt et al. 2009; Ursell et al. 2009; Silva et al. 2009; Lundbaek et al. 2004). Of particular interest is the effect that sterols present on the bilayer have on the latter (Eggeling et al. 2009; Pan et al. 2009; Epshtein et al. 2009; Qiu et al. 2009). Polyene antibiotics such as nystatin (Nys) and amphotericin B (AmB) have been studied for more than five decades (Hazen and Brown 1950; Dutcher et al. 1959) precisely because of their known dependence on sterol presence in the membrane. Interest in these molecules is mostly derived from their sustained medical use in systemic fungal infections through induced permeability of the cellular membrane, which has undesirable collateral toxicity (Hartsel and Bolard 1996; Borgos et al. 2006). Over half a century ago, it was proposed that the drug acted via the assembly of pores in the membrane (Andreoli 1974; Finkelstein and Holz 1973; de Kruijff and Demel 1974). These pores facilitated the loss of K^+ from the cell interior, finally leading to cell death (Brown et al. 1953; D'Arcy and Scott 1978). Furthermore, it was thought that the difference in the potency on membranes containing ergosterol (erg) or cholesterol (chol) was due to the influence that sterol had on the molecular structure of the pores (Dennis et al. 1970; Cass et al. 1970). This was supported by the facts that increasing amounts of sterol in the membrane lead to increasing ion permeability (de Kruijff et al. 1974a; Marty and Finkelstein 1975), that drug potency is higher in cells and model membranes when erg is present instead of chol (Dennis et al. 1970; Kinsky 1963), that bacteria are insensitive to these polyenes (D'Arcy and Scott 1978) and that the sterols added to the aqueous medium of in vitro experiments compete for the polyene and therefore diminish the effects these drugs have on sensitive organisms (Gottlieb et al. 1958). These observations have contributed to the acceptance of the polyene antibiotics action model based on direct participation of sterol in the polyene channel. However, there are experimental observations that do not entirely agree with this proposal and alternative hypotheses have emerged (Cotero et al. 1998; Venegas et al. 2003; Romine et al. 1977; Vertut-Croquin et al. 1983).

J. González-Damián · I. Ortega-Blake (✉)
Intituto de Ciencias Físicas, Universidad National Autónoma de México, Cuernavaca, Morelos, Mexico
e-mail: ivan@fis.unam.mx

J. González-Damián
Facultad de Ciencias, Universidad Autónoma del Estado de Morelos, Cuernavaca, Morelos, Mexico

It has been shown that (1) increasing mol fraction of sterol in lipid bilayers does not always lead to an increased permeability and, in the case of bilayers in the gel phase, the opposite effect has been observed (Hsuchen and Feingold 1973a, b); (2) in the absence of sterols in the membrane, polyenes are able to produce K^+ leakage (Cotero et al. 1998; Hsuchen and Feingold 1973a, b; Bolard et al. 1980; Whyte et al. 1989; Huang et al. 2002) and the channels of AmB observed in the presence or absence of sterols have the same conductances, suggesting a similar supramolecular structure (Cotero et al. 1998; Venegas et al. 2003); (3) the action of the drug seems to depend on its aggregation form in solution, and the type of sterol present in the membrane determines whether monomers, dimers or larger aggregates are required for insertion into the membrane (Huang et al. 2002; Balakrishnan and Easwaran 1993); (4) AmB is quite sensitive to membrane structure (Hsuchen and Feingold 1973a, b; Bolard et al. 1980; Whyte et al. 1989; Huang et al. 2002; Zumbuehl et al. 2004; Cohen 1992); (5) adsorption of AmB to the membrane depends on sterol presence or absence (Huang et al. 2002; Milhaud et al. 2002); (6) temperature modulates the effect of AmB in a fashion that resembles sterols (Venegas et al. 2003; de Kruijff et al. 1974b; Lambing et al. 1993; Bolard and Cheron 1982); and (7) the action of Nys is affected in a discrete manner by variations in the concentration of sterol (Wang et al. 2004). These observations have led to the search for an alternative model in which the modulation effect of sterol content on the membrane structure is responsible for selectivity (Cotero et al. 1998; Venegas et al. 2003).

Biomembranes are complex fluids formed by multiple lipids and proteins arranged in a nonrandom fashion, the components of which are able to segregate either in a uniform or a nonuniform way (Feigenson 2007, 2009; Pan et al. 2008; Engelman 2005). The segregation tendency of proteins in the lipid environment due to protein–protein interactions has been studied in the context of signaling pathways or the lipid-mediated interactions (White 2009; de Meyer et al. 2008). Recently, the lateral distribution of lipids has been addressed, and there have been substantial efforts to understand the biological role of said segregation in living cells, particularly in the case of chol (Eggeling et al. 2009; Maxfield and Mondal 2006). This interest has led to determining the phase diagrams of different mixtures of lipids and the influence of the different phases of the membrane in biologically relevant mechanisms (Feigenson 2009; Davis et al. 2009; Wagner et al. 2008; Elliott et al. 2006; Veatch and Keller 2003; de Almeida et al. 2003).

With respect to Nys, it has been shown that it is able to sense changes in the chol mol fraction of lipid membranes (Cass et al. 1970; Wang et al. 1998; Andreoli and Monahan 1968) in consonance with the proposal that membrane structure affects the drug activity. In the companion paper, Nys is shown to present two different mechanisms of ion permeation, a membrane disruption mechanism and the formation of pores. The ratio antibiotic/total lipid (in mol/mol) for the surge of the permeability through the first mechanism is 1.33×10^{-4} in the erg-containing membranes but 6.65×10^{-4} for the onset of the second mechanism, which also occurs in the chol-containing membranes at 2.0×10^{-3}; ion permeability increases exponentially after these thresholds. The companion paper reports evidence against the assumption that erg is just responsible for a greater stability of the pores formed in erg-containing membranes vis-à-vis those in chol-containing ones: A greater number of events also appear in chol-1-palmitoyl-2-oleoyl-*sn*-glycero-3-phosphocholine (POPC) membranes. The alternative idea that membrane structure is responsible for both an increase in the number of events and lifetime is supported. Here, additional evidence is provided by determining Nys activity along the phase diagrams of erg- and chol-containing POPC membranes (Silva et al. 2006). As an antecedent, we can mention the recent results of Romero et al. (2009), who found a change in the temperature dependence of AmB activity in human erythrocytes, which correlates with the change in fluidity occurring in this membrane at 18°C (Galla and Luisetti 1980).

The results of this and the companion paper are totally congruent with the Finkelstein and Holz (1973) model (FH model) for the pore structure, and they also support the idea that sterols, through a modulatory effect on the membrane structure, are responsible for regulating polyene adsorption, insertion and pore formation, rather than just acting as promoters of stave in the barrel. This latter conception is more in accordance with recent observations on the role of sterols (Feigenson 2009; Sasaki and White 2009).

Materials and Methods

Materials

POPC dissolved in chloroform and powdered chol were purchased from Avanti Polar Lipids (Alabaster, AL) and stored in the dark at −18°C. Nys was purchased from Sigma-Aldrich (Toluca, Mexico), stored at 4°C under vacuum and used without further purification. Sealed vials of erg dissolved in chloroform were purchased from Supelco (Bellefonte, PA) and stored at 4°C in the dark. Dimethyl sulfoxide (DMSO, synthesis grade), potassium chloride (KCl, ACS grade) and calcium chloride ($CaCl_2$, ACS grade) were purchased from Merck (Naucalpan, Mexico). All organic solvents were ACS grade and were purchased from J. T. Baker (Xalostoc, Mexico). Borosilicate glass capillaries were obtained from World Precision Instrument

(Sarasota, FL). High-purity nitrogen gas was supplied by Praxair (Cuernavaca, Mexico).

Small Unilamellar Vesicle Preparation

POPC, chol and erg were stored at −20°C and used without further purification. Stock chloroform solutions for every lipid were prepared once a week and stored at −20°C. Chol or erg was mixed with POPC to obtain the desired mol fraction of sterol. Evaporation of the solvent was done in a rotative evaporator (B-177; Büchi Labortechnik, Flawil, Switzerland). The suspension was prepared by adding the working solution (2 M KCl, 2 mM $CaCl_2$, 10 mM HEPES [pH 8.0]) to the film deposited in the flask and then treated in an ultrasonic bath to produce dispersion and obtain unilamellar vesicles (Paternostre et al. 1996). The suspension was stored for 2 h under refrigeration (4–6°C) prior to Nys incorporation. Eight different mol% fractions for every sterol were tested: 0.0, 7.5, 15.0, 22.5, 30.0, 37.5, 45.0 and 50.0. In all the preparations the total amount of lipids (POPC + sterol) was kept constant (7.5 μmol).

Nys Incorporation

Powdered Nys was stored at −18°C and used without further purification. A stock solution (1 mM) of Nys in methanol was prepared and used the same day. In order to homogenize, the sample of Nys in the solvent was subjected to ultrasonic dispersion. The proper amount of the stock solution of the polyene was added to the small unilamellar vesicle (SUV) preparation in order to obtain the desired concentration. The amount of Nys present in the membrane will depend not only on the concentration in solution but also on the molar ratio Nys/total lipid. The molar ratios used were 6.65×10^{-4} for erg-POPC and 2.0×10^{-3} for chol-POPC membranes. The maximal methanol fraction was 2.5% vol/vol. Homogenized suspension was obtained via ultrasonic dispersion in an N_2-enriched atmosphere after adding the polyene. The antibiotic-liposome microemulsion was then immersed in an ultrasonic bath for 15 min and stored at 4°C for 24 h before use in an N_2-enriched atmosphere.

Micropipette Fabrication

Glass capillaries with filament (1.00 mm external diameter and 0.58 mm internal diameter) from World Precision Instruments were pulled using the P2000 instrument from Sutter (Novato, CA). Micropipettes were then filled with the same working solution used for the preparation of SUVs and used within the following 20 min. The average resistance of micropipettes in the working solution was 100 ± 15 MΩ.

Solvent-Free Tip-Dip Lipid Bilayer Formation

A sample of the SUV was put in a controlled-temperature chamber, where the oxygen excess was removed by a continuous nitrogen flux. The sample was settled for 10 min at the desired temperature, and then a bilayer was formed at the tip of the micropipette by consecutive immersion in SUV suspension until a capacitive response to the square potential applied was observed (Coronado and Latorre 1983; Suarez-Isla et al. 1983). The standard seals obtained in this manner were of ∼100 GΩ with current root mean-square (I_{rms}) ∼ 0.12 pA and a 2-kHz low pass filter. The chamber was electrically insulated with a Faraday cage and suspended in elastic bands to reduce the mechanical vibration. The current signal was amplified with an Axopatch 200B and digitally converted with a Digidata 1320, both from MDS Analytical Technologies (Toronto, Canada), and stored in a personal computer. The signal was acquired with the aid of Axoscope 8.3 software from MDS Analytical Technologies at a frequency of 100 kHz. The potential applied in all of the experiments was 100 mV. It could be thought that channel formation by this protocol would include double-sided pores (Marty and Finkelstein 1975) or pores with different orientation resulting from the presence of Nys on both sides of the membrane. However, this is not the case, as has been shown in the companion paper. Also, care has to be taken in order to be sure that experiments are being done in an equilibrium situation. We determined the time average conductance as a function of time and discovered that this property needs 15 min to attain equilibrium.

Electrical Measurements

Electrical measurements were done with the Axopatch 200B amplifier from Molecular Devices (Union City, CA) set to voltage-clamp mode, 2-kHz low pass filter and maximal scaling output. The bilayer seal and pipette resistance were measured by applying a square 5-mV step potential. The signal was digitalized using a Digidata 1200A, stored and visualized in a personal computer using the software PClamp 8.2 (both from Molecular Devices). The sampling rate was set to 20 μs. Once the seal was formed, the I_{rms} obtained consistently was 0.15 ± 0.03 pA.

Time- and Lipid Phase-Dependent Experiments

Time series showing the evolution of Nys activity for 1 h were performed in POPC + 30 mol% cholesterol at 27.5°C. Once the equilibration time was determined, five different temperatures—15, 20, 25, 30 and 35°C—and eight sterol mol% fractions—0.0, 7.5, 15.0, 22.5, 30.0, 37.5, 45.0 and 50.0—were used for sampling the phase

diagram of the mixtures, with a total of 40 points. For every five experiments were performed and the time analyzed corresponded to 5 min each in an equilibrium situation (i.e., after throwing out the first 15 min of transients).

Data Analysis

All records were a posteriori baseline-corrected and digitally filtered at 1 kHz. The different conductance levels were defined following the steps suggested by Qin (2004); i.e., segments of 30 s were idealized using a model with currents defined every 0.05 pA and the segmental k-means algorithm implemented in the free software QuB (www.qub.buffalo.edu/wiki/index.php/Main_Page) (Qin et al. 1996; Qin 2004). The occupancies thus obtained, defined as the ratio of the time expended in one state to the total time of experiment, were binned; and the resulting histogram was fitted to a function composed by the sum of several gaussian terms with the aid of the fitting program included in QuB. The maximum of each gaussian term was selected as a putative conductance level. The levels obtained in this way were binned and tested for independence with a confidence interval of 95%. Those levels that presented significant dependence were eliminated, and the procedure was repeated until convergence was attained. The conductances selected provided the model from which idealizations were done. Lifetimes and number of events for each type of channel were obtained from the idealization. All graphics were done with Origin 7.5 software, purchased from OriginLab (Northhampton, MA).

For each experiment, the time average conductance change occurring in the membranes upon Nys addition was obtained from the following expression:

$$\langle G \rangle = \sum \langle G_i \rangle = \frac{\sum g_i l_i n_i}{t_{\text{exp}}} \quad (1)$$

where the index runs over the different types of channels observed, $\langle Gi \rangle$ is the time average conductance of channel type i, g_i is the actual conductance of channel type i, l_i is the lifetime of channel type i, n_i is the number of events of channel type i and t_{exp} is the time duration of the record analyzed.

Results and Discussion

Figure 1 presents examples of Nys channels appearing for the condition of no sterol in the POPC membrane. Similar to the case of AmB channels (Venegas et al. 2003), the unitary conductances are very similar to those that appear in the presence of sterols, even if the activity is much reduced (see, e.g., those at Fig. 2). This confirms that polyene channels in the absence of sterols are not protochannels (Cohen 1998) but bona fide channels that do not require sterol for their formation.

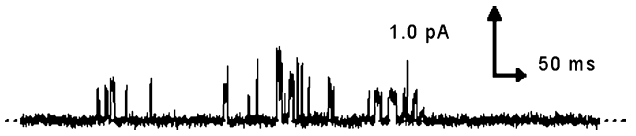

Fig. 1 Example of a continuous segment of a record of Nys channels (15 μM) in a POPC membrane without sterol. The applied voltage was 100 mV and the temperature was 15°C. *Dashed line* stands for the closed state

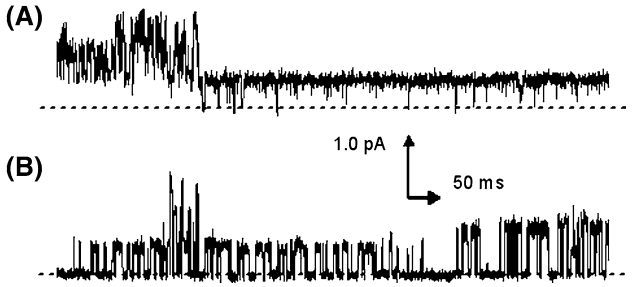

Fig. 2 Examples of a continuous current trace of Nys channels in a POPC membrane with (**a**) 30 mol% ergosterol and 30°C and (**b**) 30 mol% cholesterol at 30°C. These two conditions correspond to the respective maxima of activity for both membranes. The voltage applied was 100 mV and the open and closed states are indicated. *Dashed line* stands for the closed state

Figure 2 presents examples of the activity of Nys when a potential of 100 mV is applied to bilayers composed of POPC + 30 mol% erg at 25°C with a 6.65×10^{-3} Nys/lipid mol ratio (5/M in solution) (Fig. 2a) and POPC + 45 mol% chol at 15°C with 2.0×10^{-3} Nys/lipid mol ratio (15× M in solution) (Fig. 2b). These experimental conditions correspond to those with the greatest activity in erg- and chol-containing POPC phase diagrams. The difference in channel dynamics between the two cases is quite clear.

Figures 3 and 4 show the contour plots on a surface of temperature vs. sterol content for the average conductance change as defined in Eq. 1. The lines defining the phase diagram presented by Silva et al. (2006) are plotted in these figures. To the left of the first segmented line is the liquid disorder phase (l_d), the region between the two segmented lines is the liquid order + liquid disorder phase ($l_d + l_o$) and that to the right of the second segmented line is the liquid order phase (l_o).

The same scale was used in both figures in order to highlight the differences in activity. It is quite clear that polyene activity is correlated to the phase diagram, more so for erg than for chol. In both cases maximal activity occurs in the ($l_d + l_o$) phase, in agreement with the proposal of Zumbuehl et al. (2004) that AmB has a preference for the phase where l_o and l_d coexist; and indeed, the maxima for

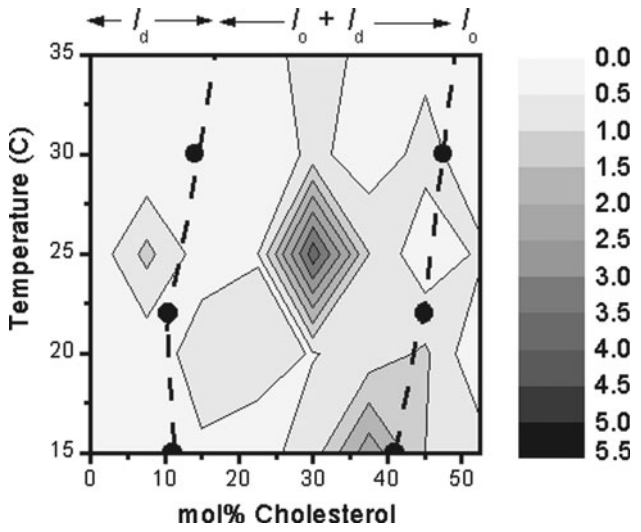

Fig. 3 Contour plot for the time average conductance (G), as defined in Eq. 1, induced by Nys in cholesterol-containing POPC membranes in a surface defined by different temperatures and sterol contents. The values for the mol fraction of sterol used were 0.0, 7.5, 15.0, 22.5, 30, 37.5, 45 and 50 mol%. Five different temperatures were selected: 15.0, 20.0, 25.0, 30.0 and 35.0°C. The segmented line and point circles correspond to the interphases obtained from the phase diagram for POPC membranes with cholesterol, as reported by Silva et al. (2006). The values considered for plotting the lines were 10.5%, 22°C; 11%, 15°C; 14%, 30°C; 17%, 40°C; 41%, 15°C; 45%, 22°C; 47.5%, 30°C; and 49%, 40°C even if some of them do not appear in the figure. The liquid ordered (l_o), liquid ordered plus liquid disordered phase ($l_o + l_d$) and liquid disordered (l_d) phases are indicated. The G values in the scale are in picosiemens. The applied voltage in all cases was 100 mV

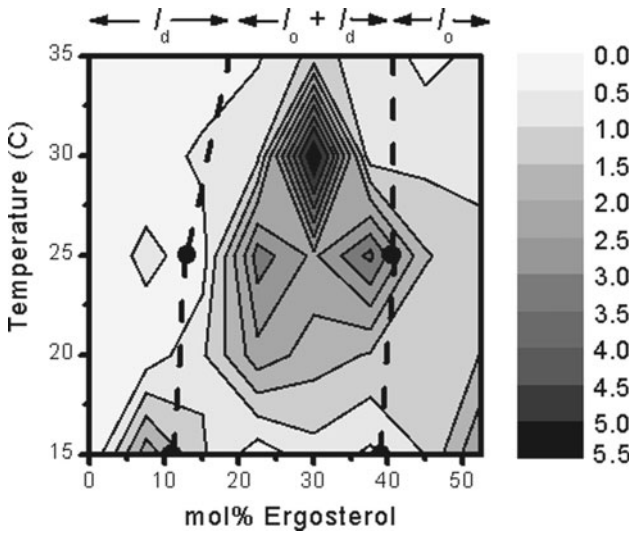

Fig. 4 Contour plot for the time average conductance (G), as defined in Eq. 1, induced by Nys in ergosterol-containing POPC membranes in a surface defined by different temperatures and sterol contents. The values for the mol fraction of sterol used were 0.0, 7.5, 15.0, 22.5, 30, 37.5, 45 and 50 mol%. Five different temperatures were selected: 15.0, 20.0, 25.0, 30.0 and 35.0°C. The segmented line and point circles were obtained from the phase diagram for POPC membranes with ergosterol, as reported by Silva et al. (2006). The values considered for plotting the line were 11%, 15°C; 13%, 25°C; 14%, 37°C; 16%, 50°C; 39%, 15°C; 40.5%, 25°C; 41%, 37°C; and 38%, 50°C even if some of them do not appear in the figure. The liquid ordered (l_o), liquid ordered plus liquid disordered phase ($l_o + l_d$) and liquid disordered (l_d) phases are indicated. The G values in the scale are in picosiemens. The applied voltage in all cases was 100 mV

both cases are located in the middle of such a phase. At low temperature (15°C) there is a local maximum in the chol-POPC membrane quite close to the boundary between the l_o and ($l_o + l_d$) phases. A similar behavior occurs for the erg-POPC membrane but now at the ($l_o + l_d$)/l_d interphase. If we take into account that erg addition results in a more ordered membrane, as chol addition, (Urbina et al. 1995), the results suggest that interphase fluctuations ($l_d/l_o + l_d$) in erg-POPC induces activity and that a similar phenomenon occurs at the ($l_o/l_o + l_d$) interphase in chol-POPC. Most important, there is a range of temperature and sterol concentrations where there is a reversed selectivity; i.e., the activity in the chol-POPC membrane is larger that in the erg-POPC one. This reversed selectivity occurs between 35 and 40 mol% of sterol and 15 and 20°C. This observation does not support the idea that erg simply gives more stability to the Nys channel.

At 25°C there is a peculiar behavior. Local extremes are present in both membranes. In both, the interphase between $l_o/(l_o + l_d)$ induces a local maximum. At the middle of the ($l_o + l_d$) phase, local maxima occur for erg-POPC, with the maximum at 30°C and 30 mol% sterol (somewhat remarkably, this results in a physiological condition). For chol-POPC the maximum occurs at 25°C and 30 mol%, whereas now a local minimum occurs at the ($l_o + l_d$)/l_d interphase, contrary to what happened at 15°C. This very rich and distinct behavior involving erg-POPC or chol-POPC demonstrates the dependence of polyene action on membrane structure and, possibly, that action is favored in the region of interphase, which could be domain boundaries.

In addition to the profile of the average conductance produced by Nys on the membrane, the behavior of single-channel properties can be assessed. In agreement with the companion paper, unitary channel conductance variations fall within the standard error, so the supramolecular arrangement does not seem to be affected by membrane structure. On the other hand, as hypothesized in the companion paper, lifetime and occupancy certainly are. In Figs. 5 and 6, the values for the lifetime of the most frequent channel (type I) along the surface temperature vs. sterol content are presented for chol-POPC and erg-POPC, respectively. It is clear that lifetime is correlated to membrane structure. In this case there is a broad maximum in the ($l_d + l_o$) phase for erg-POPC, but there is also a region of large lifetime in the region of low temperature and high sterol content. On the other hand, in the case of chol-POPC,

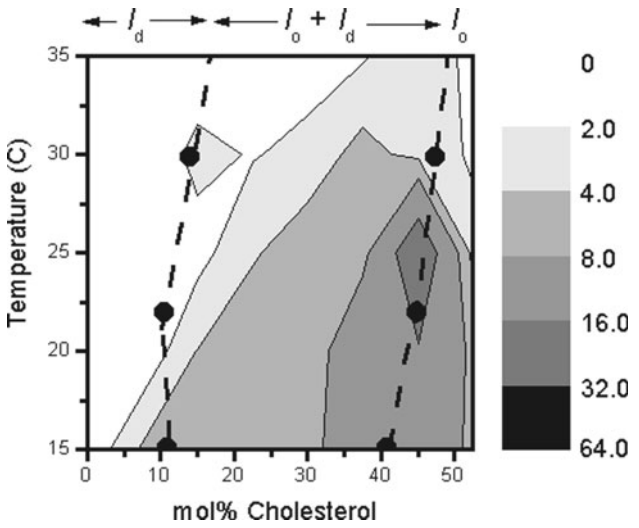

Fig. 5 Contour plot of the lifetime of channel type I in the same surface for cholesterol-containing POPC membranes presented in Fig. 3. The lifetime values in the scale are in milliseconds and the applied voltage in all cases was 100 mV

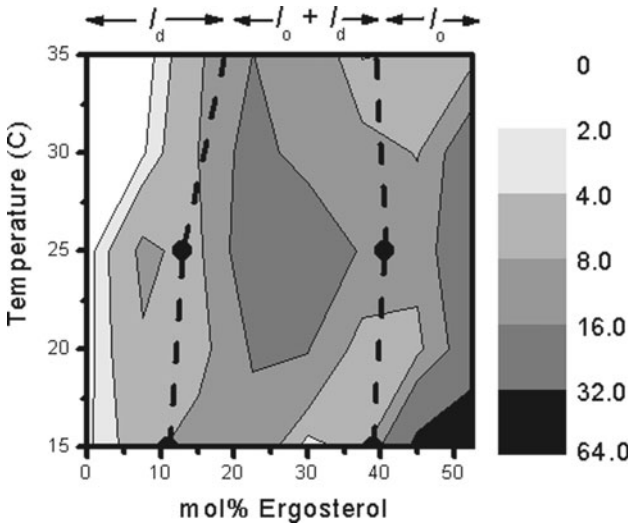

Fig. 6 Contour plot of the lifetime of channel type I in the same surface for ergosterol-containing POPC membranes presented in Fig. 4. The lifetime values in the scale are in milliseconds. The applied voltage in all cases was 100 mV

only one maximum occurs, at the interphase of the l_d/($l_o + l_d$), at 25°C. Interestingly, in this condition a local minimum is observed for the activity, which highlights the fact that the two phenomena are not correlated. Furthermore, the maximum lifetime value for erg-POPC is 45.8 ± 5.9 ms at 45% erg and 15°C. In these conditions, the corresponding value for chol-POPC is 15.5 ± 1.8 ms, showing the presumed increase in lifetime. However, the maximum lifetime for chol-POPC at 45% cholesterol and 25°C is 22.5 ± 4.7 ms and the corresponding lifetime at these conditions in erg-POPC is 10.3 ± 4.3 ms, which is substantially shorter. This eliminates the possibility that erg simply induces more stable channels.

High temperature can be expected to reduce the activity of Nys because thermal noise can hamper the formation and stability of the pores; low temperature can also reduce activity because of hindrance of the incorporation of polyene into the membrane and a reduced motility in it. Both effects are observed in Figs. 3 and 4. However, the strong correlation of activity with the phase diagram strongly supports the idea that polyene selectivity for chol- vs. erg-containing membranes comes from membrane structure, which is modulated by the sterols. This conclusion is supported by the findings reported in the companion paper, particularly that the membrane disruptions present in the erg-POPC membranes at low Nys concentrations do not appear in the chol-POPC ones. Matsumori et al. (2009) argue against this based on their recent results on the mobility of AmB in erg-POPC and chol-POPC membranes. It is clear that AmB hinders the diffusional motion of erg and, at the same time, increases its mobility in the chol-POPC membrane. On the other hand, chol mobility is not affected by AmB and neither is the mobility of AmB in chol-POPC membranes. First of all, we must note that the molar ratio between erg:AmB:POPC used in their work (1:1:18) indicates a very large polyene/total lipid ratio when compared to the one corresponding to the maximal Nys concentration that could be used without patch rupture in our work (45:1:105). This is possible because they used multilamellar vesicles instead of unilamellar ones. Very different mechanisms (a ratio of 0.05 vs. 0.007) could hence be occurring under these conditions. This is also supported by the fact that their work was done at 30°C with a very low sterol concentration (i.e., at the left-hand corner of the phase diagrams, where both erg-POPC and chol-POPC membranes present very low activity). Nonetheless, if we assume that their results reflect a general behavior, the evidence shows that there is a direct interaction between erg and AmB, whereas there is none between chol and AmB. Matsumori et al. (2009) have taken this as conclusive evidence regarding the direct role of sterol in polyene activity, and they claim that the long-standing dispute has been settled. However, AmB channels occur in spite of the lack of interaction between AmB and chol, meaning that direct interaction is not a prerequisite. As shown in this and the companion paper and contrary to what has been proposed by Prieto and coworkers (Silva et al. 2006), the difference in interaction not only affects the stability of the channels. In addition, this paper presents clear and direct evidence regarding the role of membrane structure on polyene activity. Thus, it could be claimed that membrane structure is important even when

not excluding the fact that an increased stability affects selectivity.

How can this apparently contradictory evidence be reconciled? One could present the ad hoc hypothesis that, in the erg-POPC l_d phase AmB has an intermediate mobility that hinders the large mobility of erg in this membrane, whereas the chol-POPC l_d phase does not allow for AmB mobility and, therefore, leaves chol mobility unaffected. Alternatively, one can assume that membrane structure determines the different interactions between all components of the mixture or vice versa, leading to different expressions of polyene activity. However, since lipid and sterol determine membrane structure, one can assume that the latter mostly determines polyene interactions and, thus, membrane selectivity. It would be interesting to know what the mobilities of AmB and sterols along the phase diagrams are, mainly in the points of extreme polyene activity. The results of these papers, as well as the advanced point of view, are congruent with the molecular FH model. Membrane structure can affect the activity of polyene pores, through diffusion, absortion, partition or modification of the stability in the sterol cleft proposed in the FH model.

These findings are important for understanding the molecular action of polyenes and, more generally, support the findings that membrane structural properties affect the action of biological processes, e.g., in antibiotic peptides (Huang 2009), biological channels (Schmidt et al. 2009), prions (Zhong et al. 2009), capsid assembly (Barrera et al. 2008) and fusion of membranes (Qiang and Weliky 2009; Adams and Kwon 2004).

Acknowledgements This work was supported by Consejo Nacional de Ciencia y Tecnología (24205) and Programa de Apoyo a Proyectos de Investigación e Inovación Tecnológica (DGAPA IN122909).

References

Adams M, Kwon GS (2004) Spectroscopic investigation of the aggregation state of amphotericin nystatin B during loading, freeze-drying, and reconstitution of polymeric micelles. J Pharm Pharm Sci 7:1–6

Andreoli TE (1974) Planar lipid bilayer membranes. Methods Enzymol 32(part B):513–539

Andreoli TE, Monahan M (1968) The interaction of polyene antibiotics with thin lipid membranes. J Gen Physiol 52:300–325

Balakrishnan AR, Easwaran KR (1993) CD and NMR studies on the aggregation of amphotericin-B in solution. Biochim Biophys Acta 1148:269–277

Barrera FN, del Alamo M, Mateu MG, Neira JL (2008) Envelope lipids regulate the in vitro assembly of the HIV-1 capsid. Biophys J 94:L8–L10

Bolard J, Cheron M (1982) Association of the polyene antibiotic amphotericin B with phospholipid vesicles: perturbation by temperature changes. Can J Biochem 60:782–789

Bolard J, Seigneuret M, Boudet G (1980) Interaction between phospholipid bilayer membranes and the polyene antibiotic amphotericin B: lipid state and cholesterol content dependence. Biochim Biophys Acta 599:280–293

Borgos SEF, Tsan P, Sletta H, Ellingsen TE, Lancelin J-M, Zotchev SB (2006) Probing the structure–function relationship of polyene macrolides: engineered biosynthesis of soluble nystatin analogues. J Med Chem 49:2431–2439

Brown R, Hazen EL, Mason A (1953) Effect of fungicidin (nystatin) in mice injected with lethal mixtures of aureomycin and *Candida albicans*. Science 117:609–610

Cass A, Finkelstein A, Krespi V (1970) The ion permeability induced in thin lipid membranes by the polyene antibiotics nystatin and amphotericin B. J Gen Physiol 56:100–124

Cohen BE (1992) A sequential mechanism for the formation of aqueous channels by amphotericin B in liposomes: the effect of sterols and phospholipid composition. Biochim Biophys Acta 1108:49–58

Cohen BE (1998) Amphotericin B toxicity and lethality: a tale of two channels. Int J Pharm 162:95–106

Coronado R, Latorre R (1983) Phospholipid bilayers made from monolayers on patch-clamp pipettes. Biophys J 43:231–236

Cotero BV, Rebolledo-Antúnez S, Ortega-Blake I (1998) On the role of sterol in the formation of the amphotericin B channel. Biochim Biophys Acta 1375:43–51

D'Arcy PF, Scott EM (1978) Antifungal agents. Prog Drug Res 22: 93–147

Davis JH, Clair JJ, Juhasz J (2009) Phase equilibria in DOPC/DPPC-d62/cholesterol mixtures. Biophys J 96:521–539

de Almeida RFM, Fedorov A, Prieto M (2003) Sphingomyelin/phosphatidylcholine/cholesterol phase diagram: boundaries and composition of lipid rafts. Biophys J 85:2406–2416

de Kruijff B, Demel RA (1974) Polyene antibiotic–sterol interactions in membranes of *Acholeplasma laidlawii* cells and lecithin liposomes. 3. Molecular structure of the polyene antibiotic–cholesterol complexes. Biochim Biophys Acta 339:57–70

de Kruijff B, Gerritsen WJ, Oerlemans A, Demel RA, van Deenen LL (1974a) Polyene antibiotic–sterol interactions in membranes of *Acholeplasma laidlawii* cells and lecithin liposomes. I. Specificity of the membrane permeability changes induced by the polyene antibiotics. Biochim Biophys Acta 339:30–43

de Kruijff B, Gerritsen WJ, Oerlemans A, van Dijck PW, Demel RA, van Deenen LL (1974b) Polyene antibiotic–sterol interactions in membranes of *Acholesplasma laidlawii* cells and lecithin liposomes. II. Temperature dependence of the polyene antibiotic–sterol complex formation. Biochim Biophys Acta 339: 44–56

de Meyer FJ-M, Venturoli M, Smit B (2008) Molecular simulations of lipid-mediated protein–protein interactions. Biophys J 95:1851–1865

Dennis VW, Stead NW, Andreoli TE (1970) Molecular aspects of polyene- and sterol-dependent pore formation in thin lipid membranes. J Gen Physiol 55:375–400

Dutcher JD, Gold W, Pagano JF, Vandeputte J (1959) Amphotericin B, its production, and its salts. U.S. Patent 2,908,611, October 13

Eggeling C, Ringemann C, Medda R, Schwarzmann G, Sandhoff K, Polyakova S, Belov VN, Hein B, von Middendorff C, Schönle A, Hell SW (2009) Direct observation of the nanoscale dynamics of membrane lipids in a living cell. Nature 457:1159–1162

Elliott R, Szleifer I, Schick M (2006) Phase diagram of a ternary mixture of cholesterol and saturated and unsaturated lipids calculated from a microscopic model. Phys Rev Lett 96:098101

Engelman DM (2005) Membranes are more mosaic than fluid. Nature 438:578–580

Epshtein Y, Chopra AP, Rosenhouse-Dantsker A, Kowalsky GB, Logothetis DE, Levitan I (2009) Identification of a C-terminus

domain critical for the sensitivity of kir2.1 to cholesterol. Proc Natl Acad Sci USA 106:8055–8060
Feigenson GW (2007) Phase boundaries and biological membranes. Annu Rev Biophys Biomol Struct 36:63–77
Feigenson GW (2009) Phase diagrams and lipid domains in multicomponent lipid bilayer mixtures. Biochim Biophys Acta 1788:47–52
Finkelstein A, Holz R (1973) Aqueous pores created in thin lipid membranes by the polyene antibiotics nystatin and amphotericin B. Membranes 2:377–408
Galla HJ, Luisetti J (1980) Lateral and transversal diffusion and phase transitions in erythrocyte membranes: an excimer fluorescence study. Biochim Biophys Acta 596:108–117
Gottlieb D, Carter HE, Sloneker JH, Ammann A (1958) Protection of fungi against polyene antibiotics by sterols. Science 128:361
Hartsel S, Bolard J (1996) Amphotericin B: new life for an old drug. Trends Pharmacol Sci 17:445–449
Hazen EL, Brown R (1950) Two antifungal agents produced by a soil actinomycete. Science 112:423
Hsuchen CC, Feingold DS (1973a) Polyene antibiotic action on lecithin liposomes: effect of cholesterol and fatty acyl chains. Biochem Biophys Res Commun 51:972–978
Hsuchen CC, Feingold DS (1973b) Selective membrane toxicity of the polyene antibiotics: studies on lecithin membrane models (liposomes). Antimicrob Agents Chemother 4:309–315
Huang HW (2009) Free energies of molecular bound states in lipid bilayers: lethal concentrations of antimicrobial peptides. Biophys J 96:3263–3272
Huang W, Zhang Z, Han X, Tang J, Wang J, Dong S, Wang E (2002) Ion channel behavior of amphotericin B in sterol-free and cholesterol- or ergosterol-containing supported phosphatidylcholine bilayer model membranes investigated by electrochemistry and spectroscopy. Biophys J 83:3245–3255
Kinsky SC (1963) Membrane sterols and the selective toxicity of polyene antifungal antibiotics. Antimicrob Agents Chemother 161:387–394
Lambing HE, Wolf BD, Hartsel SC (1993) Temperature effects on the aggregation state and activity of amphotericin B. Biochim Biophys Acta 1152:185–188
Lundbaek JA, Birn P, Hansen AJ, Søgaard R, Nielsen C, Girshman J, Bruno MJ, Tape SE, Egebjerg J, Greathouse DV, Mattice GL, Koeppe RE, Andersen OS (2004) Regulation of sodium channel function by bilayer elasticity: the importance of hydrophobic coupling. Effects of micelle-forming amphiphiles and cholesterol. J Gen Physiol 123:599–621
Marty A, Finkelstein A (1975) Pores formed in lipid bilayer membranes by nystatin, differences in its one-sided and two-sided action. J Gen Physiol 65:515–526
Matsumori N, Tahara K, Yamamoto H, Morooka A, Doi M, Oishi T, Murata M (2009) Direct interaction between amphotericin B and ergosterol in lipid bilayers as revealed by ^{2}H NMR spectroscopy. J Am Chem Soc 131:11855–11860
Maxfield FR, Mondal M (2006) Sterol and lipid trafficking in mammalian cells. Biochem Soc Trans 34(pt 3):335–339
Milhaud J, Ponsinet V, Takashi M, Michels B (2002) Interactions of the drug amphotericin B with phospholipid membranes containing or not ergosterol: new insight into the role of ergosterol. Biochim Biophys Acta 1558:95–108
Pan J, Tristram-Nagle S, Kucerka N, Nagle JF (2008) Temperature dependence of structure, bending rigidity, and bilayer interactions of dioleoylphosphatidylcholine bilayers. Biophys J 94: 117–124
Pan J, Tieleman DP, Nagle JF, Kucerka N, Tristram-Nagle S (2009) Alamethicin in lipid bilayers: combined use of X-ray scattering and MD simulations. Biochim Biophys Acta 1788: 1387–1397
Paternostre M, Ollivon M, Bolard J (1996) Preparation and membrane protein reconstitution. In: Prasad E(ed) Manual on membrane lipids. Springer, Berlin
Phillips R, Ursell T, Wiggins P, Sens P (2009) Emerging roles for lipids in shaping membrane-protein function. Nature 459:379–385
Qiang W, Weliky DP (2009) HIV fusion peptide and its cross-linked oligomers: efficient syntheses, significance of the trimer in fusion activity, correlation of beta strand conformation with membrane cholesterol, and proximity to lipid headgroups. Biochemistry 48:289–301
Qin F (2004) Restoration of single-channel currents using the segmental k-means method based on hidden Markov modeling. Biophys J 86:1488–1501
Qin F, Auerbach A, Sachs F (1996) Estimating single-channel kinetic parameters from idealized patch-clamp data containing missed events. Biophys J 70:264–280
Qiu L, Lewis A, Como J, Vaughn MW, Huang J, Somerharju P, Virtanen J, Cheng KH (2009) Cholesterol modulates the interaction of beta-amyloid peptide with lipid bilayers. Biophys J 96:4299–4307
Romero EA, Valdivieso E, Cohen BE (2009) Formation of two different types of ion channels by amphotericin B in human erythrocyte membranes. J Membr Biol 230:69–81
Romine WO, Sherette GR, Brown GB, Bradley RJ (1977) Evidence that nystatin may not form channels in thin lipid membranes. Biophys J 17:269–274
Sasaki H, White SH (2009) A novel fluorescent probe that senses the physical state of lipid bilayers. Biophys J 96:4631–4641
Schmidt D, Cross SR, MacKinnon R (2009) A gating model for the archeal voltage-dependent K^{+} channel kvap in DPhPC and POPE:POPG decane lipid bilayers. J Mol Biol 390:902–912
Silva L, Coutinho A, Fedorov A, Prieto M (2006) Competitive binding of cholesterol and ergosterol to the polyene antibiotic nystatin: a fluorescence study. Biophys J 90:3625–3631
Silva LC, Futerman AH, Prieto M (2009) Lipid raft composition modulates sphingomyelinase activity and ceramide-induced membrane physical alterations. Biophys J 96:3210–3222
Suarez-Isla BA, Wan K, Lindstrom J, Montal M (1983) Single-channel recordings from purified acetylcholine receptors reconstituted in bilayers formed at the tip of patch pipets. Biochemistry 22:2319–2323
Urbina JA, Pekerar S, Le HB, Patterson J, Montez B, Oldfield E. (1995) Molecular order and dynamics of phosphatidylcholine bilayer membranes in the presence of cholesterol, ergosterol and lanosterol: a comparative study using ^{2}H-, ^{13}C- and ^{31}P NMR spectroscopy. Biochim Biophys Acta 1238:163–176
Ursell TS, Klug WS, Phillips R (2009) Morphology and interaction between lipid domains. Proc Natl Acad Sci USA 106:13301–13306
Veatch SL, Keller SL (2003) Separation of liquid phases in giant vesicles of ternary mixtures of phospholipids and cholesterol. Biophys J 85:3074–3083
Venegas B, González-Damián J, Celis H, Ortega-Blake I (2003) Amphotericin B channels in the bacterial membrane: role of sterol and temperature. Biophys J 85:2323–2332
Vertut-Croquin A, Bolard J, Chabbert M, Gary-Bobo C (1983) Differences in the interaction of the polyene antibiotic amphotericin B with cholesterol- or ergosterol-containing phospholipid vesicles: a circular dichroism and permeability study. Biochemistry 22:2939–2944
Wagner K, Desbat B, Brezesinski G (2008) Liquid–liquid immiscibility in model membranes activates secretory phospholipase A_2. Biochim Biophys Acta 1778:166–174
Wang MM, Sugar IP, Chong PL (1998) Role of the sterol superlattice in the partitioning of the antifungal drug nystatin into lipid membranes. Biochemistry 37:11797–11805

Wang MM, Olsher M, Sugár IP, Chong PL-G (2004) Cholesterol superlattice modulates the activity of cholesterol oxidase in lipid membranes. Biochemistry 43:2159–2166

White SH (2009) Biophysical dissection of membrane proteins. Nature 459:344–346

Whyte BS, Peterson RP, Hartsel SC (1989) Amphotericin B and nystatin show different activities on sterol-free vesicles. Biochem Biophys Res Commun 164:609–614

Zhong J, Yang C, Zheng W, Huang L, Hong Y, Wang L, Sha Y (2009) Effects of lipid composition and phase on the membrane interaction of the prion peptide 106–126 amide. Biophys J 96:4610–4621

Zumbuehl A, Stano P, Heer D, Walde P, Carreira EM (2004) Amphotericin B as a potential probe of the physical state of vesicle membranes. Org Lett 6:3683–3686